AUT Journal of Electrical Engineering

AUT J. Electr. Eng., 56(1) (Special Issue) (2024) 95-112
DOI: 10.22060/eej.2023.22129.5518

Design Optimization of the Multi-layer Switched Reluctance Motor to Minimize Torque Ripple and Maximize Average Torque

Payam Vahedi[1], B. Ganji[1*], Seyed Ebrahim Afjei[2]

[1] Faculty of Electrical and Computer Engineering, University of Kashan, Kashan, Iran
[2] Faculty of Electrical Engineering, Shahid Beheshti University, Tehran, Iran

ABSTRACT: Because of the high torque ripple of the switched reluctance motor (SRM), a novel design optimization method is introduced in the present paper for the multi-layer switched reluctance motor. Using this design optimization method, torque ripple is reduced significantly, and average torque is increased as well. In the proposed method, the significant reduction of torque ripple is derived from variation of both the motor geometric structure and the design/control parameters. The most important design parameters of the SRM that have a significant effect on the torque ripple and average torque of the motor are stator/rotor pole arcs. The optimal values of these parameters are determined here using the design of experiments (DOE) algorithm. Having the instantaneous torque waveform of the motor is necessary for the accurate calculation of torque ripple. In the present paper, this waveform is predicted using an analysis of the motor based on finite element method (FEM). Applying the introduced design optimization method to a typical 8/6 multi-layer SRM, simulation results are presented and the effectiveness of the proposed design optimization method is demonstrated. Since the produced average torque of the multi-layer SRM is higher than the conventional type of SRM (one-layer), the proposed design optimization procedure could be utilized appropriately for the construction of a high-power SRM with minimum torque ripple.

Review History:

Received: Jan. 30, 2023
Revised: Mar. 18, 2023
Accepted: Jun. 06, 2023
Available Online: Feb. 01, 2024

Keywords:

Multi-layer switched reluctance motor
Design optimization
Torque ripple
Finite element method

1- Introduction

The SRM was introduced for the first time in 1838 but special attention was paid to it three decades ago with the development of power electronics and control algorithms [1-2]. Due to the exclusive merits of this motor such as high reliability, concentrated winding, simple and rugged structure, and appropriate operation at high-speed large-temperature conditions, it is usually selected as an appropriate candidate for different applications [3-6]. In spite of the above-mentioned advantages, torque ripple and noise in this motor are high, and many works are done by researchers to improve these two issues [7-22].

To reduce torque ripple and increase average torque, design optimization of the SRM is done in [11] and the optimum stator/rotor pole arcs are then determined. In [12], the optimization of an SRM using a multi-objective optimization method based on a genetic-fuzzy algorithm is proposed. High efficiency and low torque ripple are the objective functions of the optimization procedure in this reference. Using electromagnetic and thermal finite-element analysis (FEA), a design method of the SRM is introduced in [13] to minimize the total cost. Based on the Taguchi fractional factorial DOE, the optimization of geometrical parameters for the SRM to maximize torque is presented in [14]. By changing the geometric structure of the rotor, a different structure of the 2-layer 6/4 SRM is introduced in [15] to decrease torque ripple. In [16], an optimization design method based on the genetic algorithm for a two-phase SR compressor drive is introduced. Using flux-linkage characteristics predicted from the magnetic equivalent circuit (MEC) method, the dynamic analysis of the SRM is done in this reference. Multi-objective design optimization of the SRM for EVs is introduced in [17] to maximize average torque, average torque per copper loss, and average torque per motor volume. The stator and rotor pole arc angles are the optimized variables in this work. The design of a high-speed 2-phase 4/2 SRM for an air blower is presented in [18]. The rotor pole shape is optimized in this reference to reduce torque ripple based on a reiterative optimization algorithm using FEA.

An optimization method based on the DOE method is introduced in [19] for SRM to optimize five geometries of SRM and turn-on and turn-off angles. Based on a combination of the DOE and particle swarm optimization methods, multi-objective design optimization of the SRM is done in [20]. The optimal design of SRM for electric vehicles (EVs) is presented in [21]. Six design criteria including wide speed

*Corresponding author's email: bganji@kashanu.ac.ir

range, high efficiency, good overload capability, small torque ripple, low cost, and high power density are considered in this optimization. A constrained multi-objective optimization procedure for the design and control of a SRM based on a non-dominated sorting genetic algorithm has been introduced in [22]. This work optimizes SRM to maximize efficiency and average torque and minimize torque ripple. The factors of optimization includes air-gap length, rotor inner diameter, stator pole arc angle, rotor pole arc angle, stator pole height, and stator inner diameter as well as turn-on and turn-off firing angles. Based on the MEC method, the electromagnetic modeling of the multi-layer SRM is done in [23]. A shape design procedure is also introduced in this reference for torque ripple reduction of different types of multi-layer SRM.

Although various design optimization methods are reported for the conventional SRM, less attention has been paid to the design optimization of multi-layer SRM [15, 23]. The design optimization of the multi-layer SRM to improve torque ripple and average torque is the main objective of the present paper. In the following, the design optimization procedure proposed for the reduction of torque ripple and increase of average torque is described in section 2. Implementing this procedure to a typical multi-layer 8/6 SRM, simulation results are presented in section 3 and its effectiveness is evaluated. Finally, the paper is concluded in section 4.

2- The Proposed Design Optimization Procedure

The design optimization method proposed for the multi-layer SRM consists of two separate parts which are described in the following.

2- 1- Optimum Design Parameters

The most important design parameters of the SRM that have a significant impact on torque ripple and average torque are stator/rotor pole arcs [11]. To find the optimum values of these two parameters, it is necessary to carry out a dynamic analysis of the SRM as explained in [1]. In addition, turn-on and turn-off angles as the control parameters have a significant effect on the torque ripple and average torque of the machine. Using the DOE algorithm and doing dynamic analysis, optimum values of poles arcs and these control parameters are determined here to maximize the average torque and minimize the torque ripple. The current regulation control mode is considered in this optimization because the objective is to find the optimum values of design/control parameters for a constant current (around nominal current).

Design optimization is an important goal in any research. Different statistical methods for the optimization of parameters are used and one of them is the DOE method which is centered on factors, responses, and runs. This method is a systematic method to determine the relationship between factors affecting a process and the output of that process. Some of the most common DOE types are as follows: (1) one-factor designs, (2) factorial designs which include: general full factorial designs, two-level full factorial designs, two-level fractional factorial designs, Plackett-burman designs, Taguchi's orthogonal arrays, (3) response surface method designs, (4) reliability DOE. In the present paper, the response surface method (RSM) is used as an optimization method. The effect of each factor (the factor F) and their interactions on the response variable can be calculated using the analysis of means (ANOM). The impact of the change of the factor F from the low to the high level at the response R can be calculated as:

$$E_R(F)=\frac{\sum_{i\in F^+} R_i}{N_i}-\frac{\sum_{j\in F^-} R_j}{N_j} \quad (1)$$

where F^+ is the subset of the simulation, F takes the high level (+), N_i is the size of this subset. Similarly, F^- and N_j are the subset of simulations with F at the low level and the size of this subset, respectively. The effect of the interaction of the factors F_1 and F_2 is:

$$E_R(F_1.F_2)=\frac{\sum_{i\in(F_1.F_2)^+} R_i}{N_i}-\frac{\sum_{j\in(F_1.F_2)^-} R_j}{N_j} \quad (2)$$

where $(F_1.F_2)^+$ represents the subset of simulation with the factors F_1 and F_2 at the same level. This includes the simulation when both F_1 and F_2 are at the high level as well as the ones where they are both at the low level. In contrast, both factors are at different levels for the simulation results related to $(F_1.F_2)^-$.

2- 2- Shape Design Optimization

With regard to Fig. 1, it is seen that the rotors of different layers are completely aligned for the conventional multi-layer SRM. In other words, there is no displacement between the rotors. Since different layers in the conventional multi-layer SRM have similar performance, they produce the same torque waveforms. Therefore, the instantaneous torque of the multi-layer SRM can be easily derived from the torque waveform of one layer when the amplitude of this predicted waveform is multiplied by the number of layers. As a result, although the conventional multi-layer SRM produces more average torque in comparison to the one-layer SRM, their torque ripple is the same. Using many simulation results provided for different types of the multi-layer SRM, we have already demonstrated in [23] that torque ripple can be decreased significantly when there is a displacement between different rotors as illustrated in Fig. 1c. For different types of the multi-layer SRM, the optimum value of α angle is obtained using below equation [23]:

$$\alpha=\frac{360^\circ}{P_r N_{phase} N_{layer}} \quad (3)$$

where P_r is the number of rotor poles in each layer, N_{phase} is the number of phases in each layer and N_{layer} is the number of layers, respectively.

Table 1. Motor specifications [25]

Stator outer diameter [mm]	125
Stator slot-bottom diameter [mm]	100
Rotor outer diameter [mm]	63
Rotor slot-bottom diameter [mm]	41
Air gap length [mm]	0.35
Shaft diameter [mm]	21
Stack length [mm]	90
Stator pole arc [deg.]	21
Rotor pole arc [deg.]	21
Turns per coil	124
Nominal power [kW]	1
Nominal coil current [A]	8
Nominal speed [rpm]	1500
Resistance @ 20° C [Ω]	0.69

3- Simulation Results

In order to evaluate the effectiveness of the proposed design optimization procedure, a typical multi-layer 8/6 SRM is considered and the simulation results are presented in this section. It should be noted that every layer of the discussed multi-layer SRM is an 8/6 SRM with specifications given in Table 1. In addition, each phase of this 8/6 SRM includes two coils in parallel and the laminations of the stator and rotor are M800-50A with 0.5 mm thickness. Carrying out 2D FE transient analysis of the discussed 2-layer 8/6 SRM, the instantaneous torque of the motor is predicted for the current regulation control mode. In this analysis, the maximum current is 12 A, the hysteresis band is 0.1 A, the turn-on angle is 5°, the turn-off angle is 20°, speed is 1500 rpm, phase voltage is 500 V. The predicted instantaneous torque is illustrated in Fig. 2. It should be explained that the ANSYS finite element package is used here for the analysis of the motor.

The sequence of implementation of the two procedures described in sections 2-1 and 2-2 is important and therefore two different design optimization methods could be considered. In the first method, the design optimization procedure described in section 2-1 is applied for one layer, and the optimum values of the stator pole arc, the rotor pole arc, and the turn-on angle are obtained. Considering different layers, the impact of the design optimization procedure described in section 2-2 is then evaluated. In the second method, different types of multi-layer SRM (2-layer, 3-layer, 4-layer, …) are considered and their optimization is done using the design optimization procedure described in sections 2-2. For each optimized motor, the design optimization procedure described in section 2-1 is then applied. In the following, the simulation results related to these two methods are presented.

3- 1- The First Design Optimization Method

When the discussed 2-layer 8/6 SRM is optimized using the design optimization procedure described in section 2-1, the optimum values of the stator pole arc, the rotor pole arc, and the turn-on angle are 23.7°, 22.5°, and 6.6°, respectively. For these optimum values when the conduction angle is 15°, instantaneous torque of the motor is predicted and it is shown in Fig. 3. Comparing Fig. 2 and 3, it is observed that torque ripple is reduced and average torque is also increased significantly. Having the predicted instantaneous torque, average torque, and torque ripple can be calculated and they

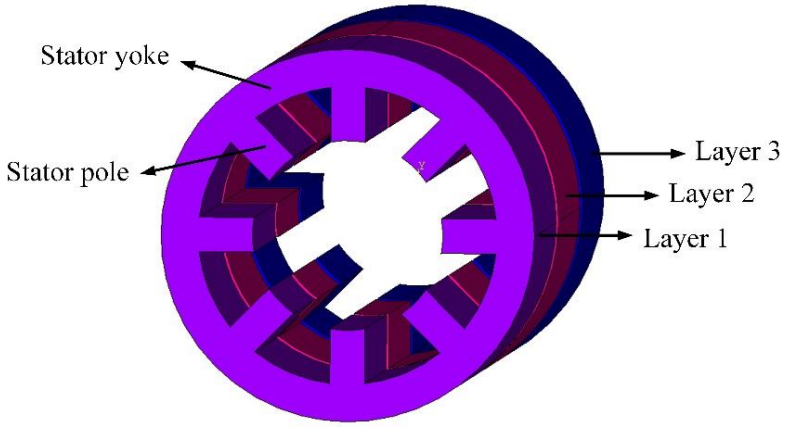

(a)

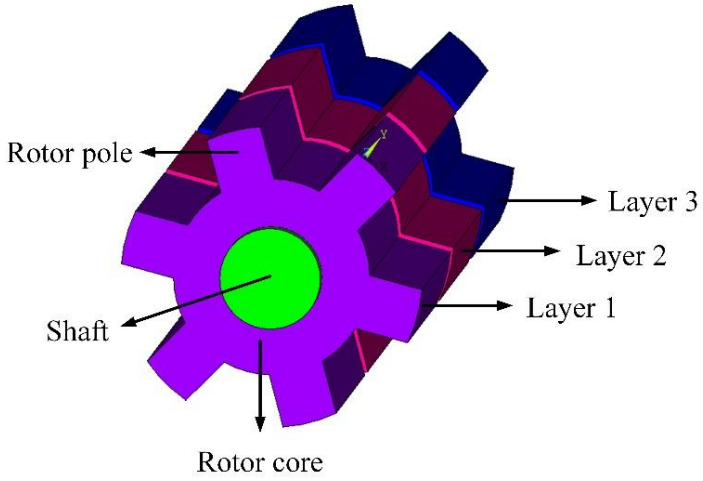

(b)

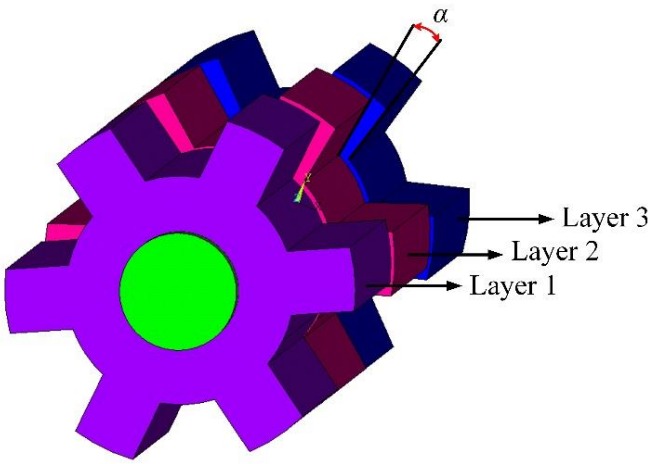

(c)

Fig. 1. The structure suggested for multi-layer SRM: (a) stator, (b) rotor of conventional structure, (c) rotor of suggested structure

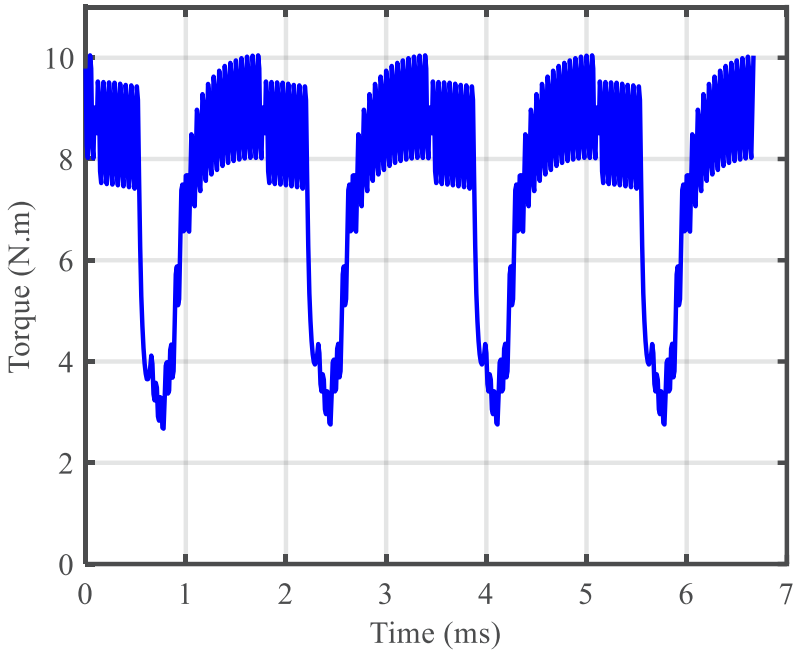

Fig. 2. Instantaneous torque of discussed 2-layer 8/6 SRM

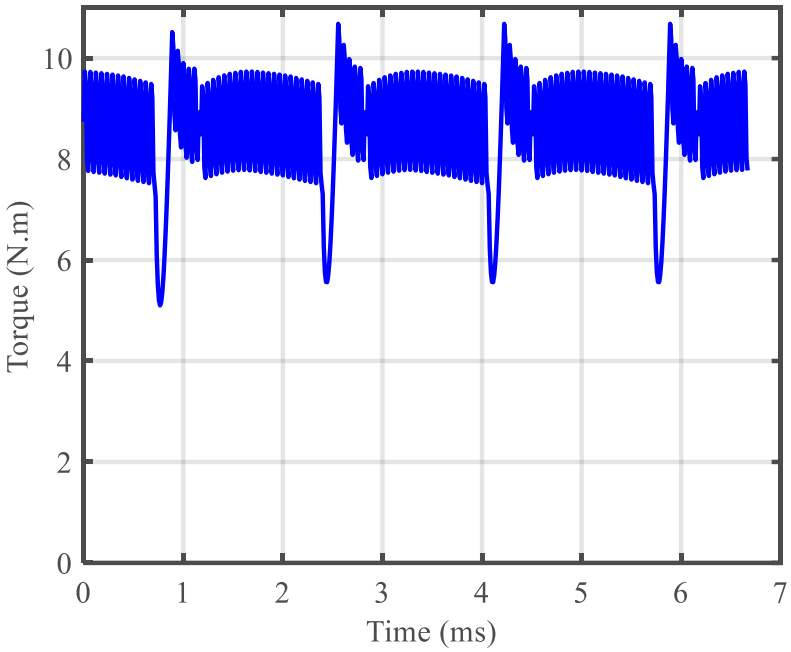

Fig. 3. Instantaneous torque of the 2-layer 8/6 SRM when the design optimization algorithm described in section 2-1 is implemented only

Table 2. Simulation results required for the considered DOE

Run order	Stator pole arc [deg.]	Rotor pole arc [deg.]	Turn on angle [deg.]	Average torque [N.m]	Torque ripple [%]
1	24	17	9	4	32.6
2	20.5	14.6	7	3.4	60.9
3	20.5	20.5	7	4	32
4	20.5	20.5	7	4	32
5	20.5	20.5	7	4	312
6	17	17	9	3.7	48.1
7	20.5	20.5	7	4	32
8	24	17	5	3.7	50.5
9	24	24	9	3.9	39.9
10	20.5	26.4	7	4.1	35.6
11	26.4	20.5	7	4.2	34.3
12	17	24	9	3.9	42.2
13	17	17	5	2.7	84.3
14	17	24	5	3.6	54.7
15	24	24	5	4.2	31.8
16	20.5	20.5	7	4	32
17	20.5	20.5	3.6	3.3	64.6
18	20.5	20.5	7	4	32
19	14.6	20.5	7	3.3	61.6
20	20.5	20.5	10.4	4.1	40.1

are 7.4 N.m and 49.7 % for Fig. 2 and 8.5 N.m and 32.7 % for Fig. 3, respectively. It must be added that the following equation is used for torque ripple calculation.

$$Torque\ ripple\ \% = \frac{T_{max} - T_{min}}{2 \times T_{avg.}} \times 100 \quad (4)$$

where T_{max} and T_{min} are maximum and minimum torque and T_{avg} is average torque.

To find the above-mentioned optimum parameters, the required simulation results of DOE are given in Table 2. It must be indicated that the DOE method has been implemented here using the Minitab software. As indicated in [11], one phase of the 8/6 SRM will ideally be excited

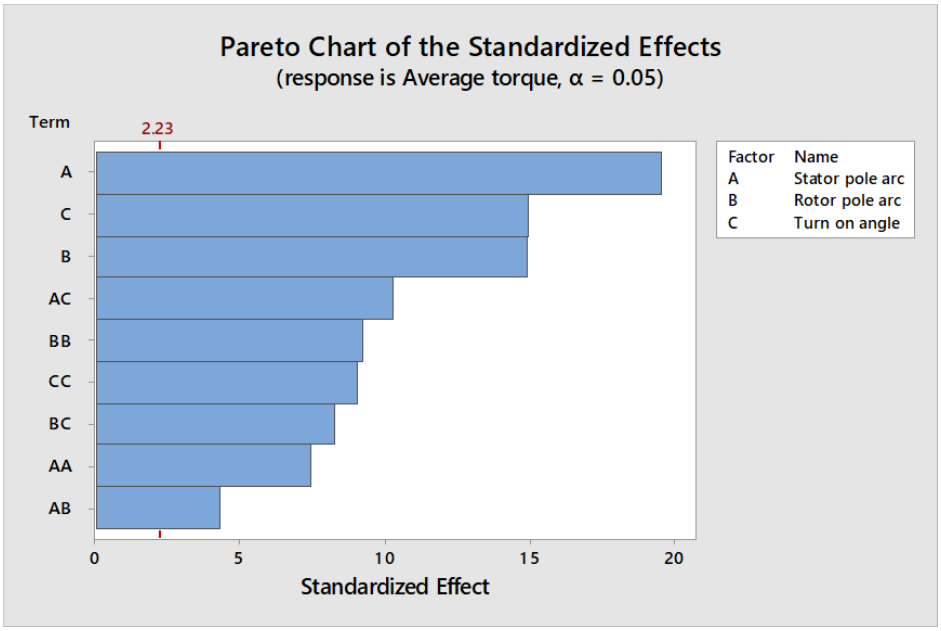

(a)

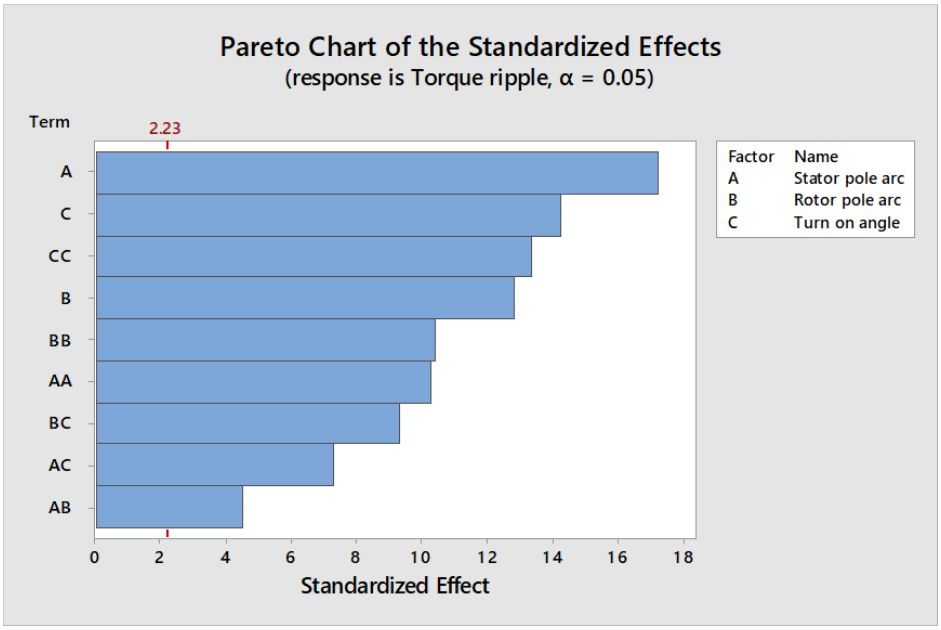

(b)

Fig. 4. Residual histograms, (a) the average torque, (b) torque ripple

for 15° only. Therefore, it is enough to concentrate on the turn-on angle as a variable parameter in the discussed design optimization. This is because the turn-off angle can be then derived from the turn-on angle (the difference between them is 15°). The residual plots related to the average torque and the torque ripple depicted in Fig. 4 can be used to verify these results. The residual plot is a graph that is used to examine the goodness-of-fit in regression and analysis of variance. Examining residual plots helps us determine whether the ordinary least squares assumptions are being met. As clear from this figure, the shape of the residual histogram has a normal distribution. This shows that the experiment's results are around their estimated values. A straight line for the points means that the residuals are distributed normally. In order to see that there is a constant variance for the residuals, the residual histogram, the residuals versus order/fits plots, and the normal plot of residuals are usually used.

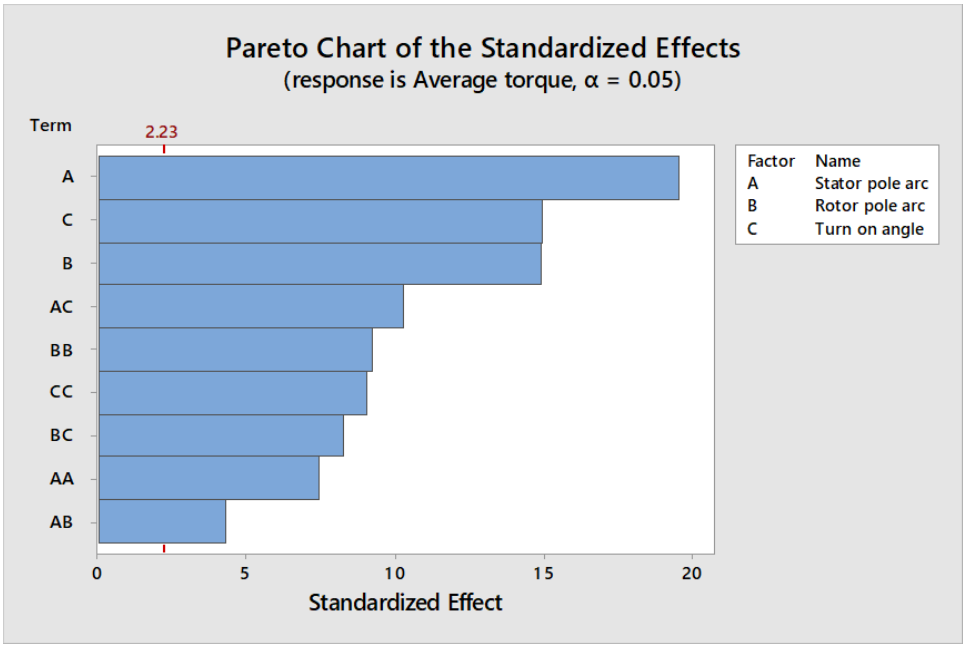

(a)

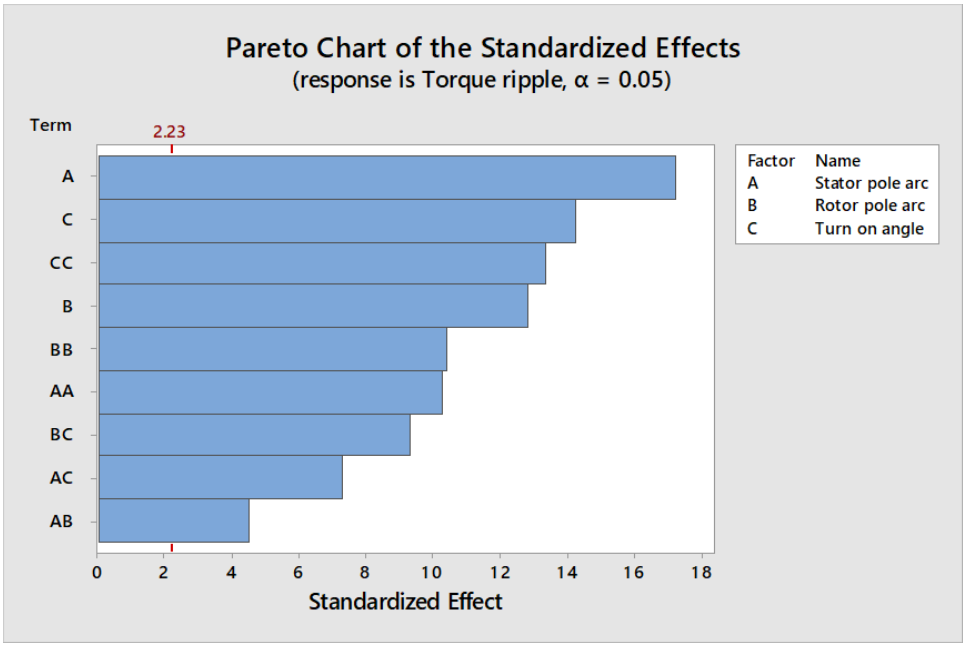

(b)

Fig. 5. Standardized effect, (a) the average torque, (b) torque ripple

The main effects of the factors including stator pole arc, rotor pole arc, and turn-on angle on the average torque and torque ripple are shown in Fig. 5 and it is clear that the effect of stator pole arc is greatest. The Pareto chart is used to indicate the magnitude and the importance of the effects. The reference line in the Pareto chart is used to indicate which effects are statistically significant. The reference line for statistical significance depends on the significance level (denoted by α). Bars of the Pareto chart, which cross the reference line, are important. In the depicted Pareto chart, the bars that represent all factors cross the reference line that is at 2.23. These factors are statistically significant at the 0.05 level with the current model terms.

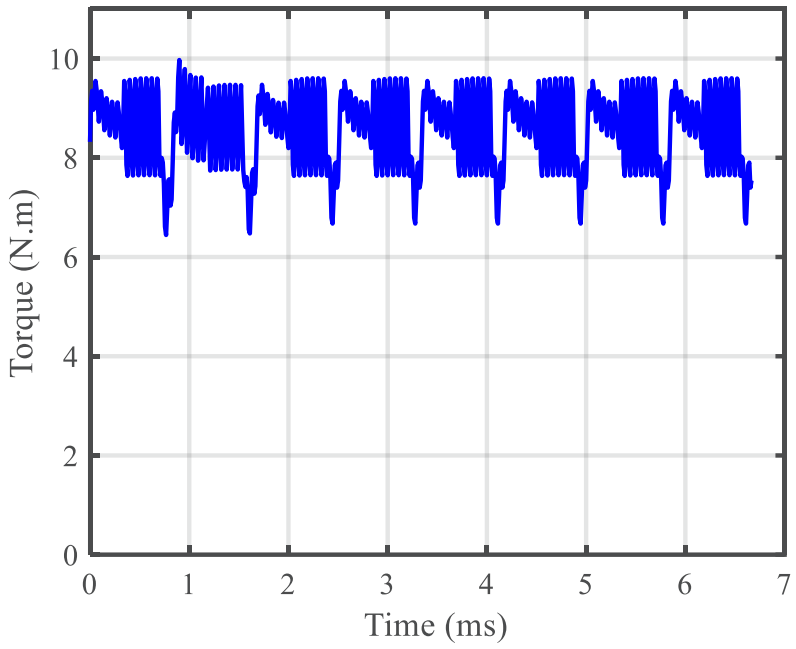

Fig. 6. Instantaneous torque of the discussed 2-layer 8/6 SRM when it is optimized by the second optimization design method

When the second part of the proposed design optimization procedure described in section 2-2 is also applied, a displacement by 7.5° between two adjacent rotors should be considered for the optimum motor where stator pole arc, rotor pole arc, turn-on angle, and turn-off angle are 23.7°, 22.5°, 6.6°, and 21.6°, respectively. In this case, the instantaneous torque of the discussed 2-layer 8/6 SRM is predicted and it is shown in Fig. 6. For this torque waveform, average torque and torque ripple are 8.5 N.m and 20.7 %, respectively. Comparing Fig. 2 and 6 shows that a significant reduction of torque ripple and increase of torque average can result using the design optimization procedure introduced in section 2.

When the number of layers in the multi-layer SRM is increased, we have a larger average torque which is the product of the average torque calculated for the one-layer SRM and the number of layers [23]. With the increase of the number of layers for the discussed multi-layer 8/6 SRM, the simulation results of different designs derived from the first method (presented separately in Figs. 2, 3, and 6 for the discussed 2-layer 8/6 SRM) are compared in Figs. 7-8 for the 3-layer 8/6 SRM and the 4-layer 8/6 SRM, respectively. The average torque and torque ripple values related to different designs are summarized in Table 3. It is added that design 1 indicates to initial design of the motor. When the multi-layer 8/6 SRM is optimized only using the design optimization procedure described in section 2-1, design 2 is resulted. Finally, design 3 is obtained when the motor is optimized using the first design optimization method. The comparison done in Figs. 7-8 and Table 3 show well that the first design optimization method proposed for the multi-layer SRM is much more effective when the number of layers is also increased.

3- 2- The Second Design Optimization Method

As indicated above, another possibility for optimization is that the design optimization procedure described in sections 2-2 is applied at first for different types of multi-layer SRM (2-layer, 3-layer, 4-layer, and …). For each optimized motor, the design optimization procedure described in section 2-1 is then used and the optimum values of the design parameters including stator pole arc, rotor pole arc, and turn-on angle are obtained. The related simulation results are presented here.

To find the optimum values of the above-mentioned design parameters for the discussed 2-layer SRM with the suggested structure introduced in section 2-2 (α=7.5°), the related DOE simulation results are summarized in Table 4. When the design optimization procedure described in sections 2-1 is applied to this motor, the stator pole arc, rotor pole arc, and turn-on angle are optimized and they are 24.2°, 21.9°, and 7.1°, respectively. For these optimum values when the conduction angle is 15°, instantaneous torque of the motor is predicted. The predicted instantaneous torque, average torque, and torque ripple can be calculated and they are 8.41 N.m and 21.69 %, respectively.

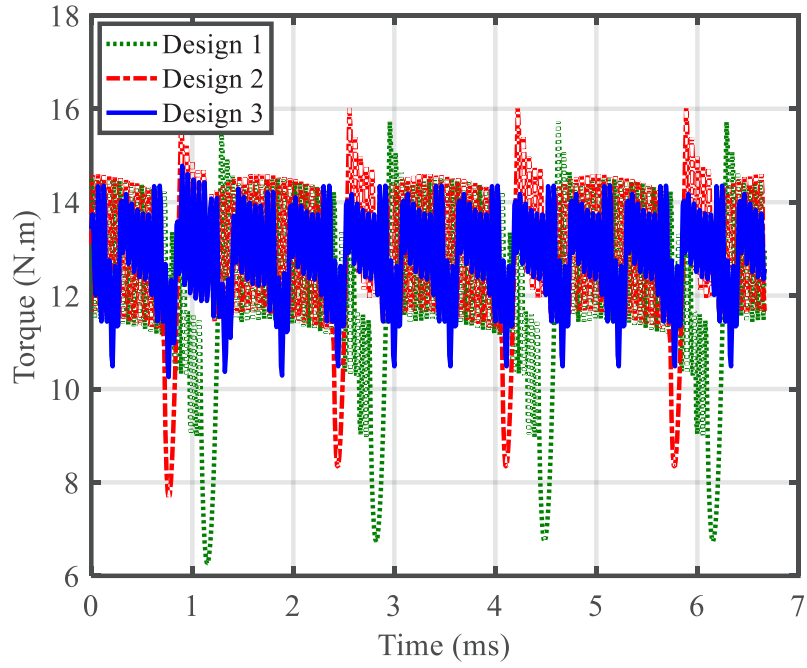

Fig. 7. Instantaneous torque of the 3-layer 8/6 SRM

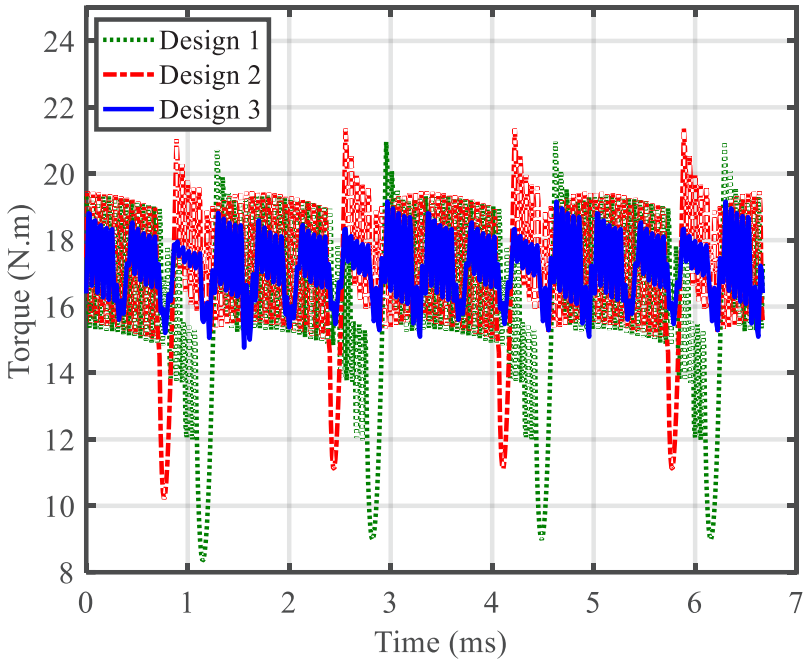

Fig. 8. Instantaneous torque of the 4-layer 8/6 SRM

Table 3. Simulation results related to the first method

		Design 1	Design 2	Design 3
2-layer SRM	Average torque [N.m]	7.4	8.5	8.5
	Torque ripple [%]	49.7	32.7	20.7
3-layer SRM	Average torque [N.m]	11.12	12.8	12.8
	Torque ripple [%]	49.73	32.7	17.7
4-layer SRM	Average torque [N.m]	14.83	17.1	17.1
	Torque ripple [%]	49.73	32.7	12.9

Similarly, the DOE simulation results required for 3-layer and 4-layer 8/6 SRM with the suggested structure described in section 2-2 are given in Tables 5 and 6, respectively. For the discussed 3-layer 8/6 SRM optimized with the design optimization procedure described in section 2-2 (α=5°), the optimal values of the stator pole arc, rotor pole arc, and turn-on angle are 26.4°, 23.8°, and 4.6°, respectively. These values are also 25.8°, 17.5° and 8.3° for the discussed 4-layer 8/6 SRM optimized with the design optimization procedure described in section 2-2 (α=3.75°).

The simulation results of different designs derived from the second design optimization method are compared in Figs. 9-11 for the 2-layer 8/6 SRM, the 3-layer 8/6 SRM, and the 4-layer 8/6 SRM, respectively. For better comparison, the values of average torque and torque ripple related to different designs are also given in Table 7. It should be explained that design 1 indicates the initial design of the motor without any optimization as defined in Table 3. When the design optimization procedure described in sections 2-2 is applied only, the design 4 is resulted. Finally, design 5 is obtained when the motor is optimized using the second design optimization method.

Another important type of SRM which is mostly utilized for different applications is the three-phase 6/4 SRM. To demonstrate the effectiveness of the proposed design optimization method, it is also applied to the multi-layer 6/4 SRM described in [23]. All design specifications of this motor except stator/rotor pole arcs are similar to those for the discussed one-layer 8/6 SRM given in Table 1. Similar to the discussed multi-layer 8/6 SRM, the stator pole arc and rotor pole arc are the same in the multi-layer 6/4 SRM and they are 28°. Applying the first design optimization method described in section 3-1 to this multi-layer 6/4 SRM, the related simulation results are obtained and they are summarized in Table 8. As explained in section 2-1, a part of the proposed design optimization method is to find the optimal values of stator pole arc, rotor pole arc, turn-on angle, and turn-off angle. For the considered multi-layer 6/4 SRM, optimal values of these parameters derived from the DOE are 34°, 34°, 8.6° and 38.6°, respectively. Comparing Table 3 and Table 8, it is seen that the proposed design optimization method is effective for other types of multi-layer SRM.

Table 4. The DOE simulation results for 2-layer 8/6 SRM with α=7.5°

Run order	Stator pole arc [deg.]	Rotor pole arc [deg.]	Turn on angle [deg.]	Average torque [N.m]	Torque ripple [%]
1	24	17	9	8.4	21
2	20.5	14.6	7	6.7	35.3
3	20.5	20.5	7	8.1	21.4
4	20.5	20.5	7	8.1	21.4
5	20.5	20.5	7	8.1	21.4
6	17	17	9	7.5	27.7
7	20.5	20.5	7	8.1	21.4
8	24	17	5	7.5	29.6
9	24	24	9	7.9	25.7
10	20.5	26.4	7	8.1	23.8
11	26.4	20.5	7	8.5	21.2
12	17	24	9	7.9	24.1
13	17	17	5	5.5	33.7
14	17	24	5	7.1	30.3
15	24	24	5	8.4	20.7
16	20.5	20.5	7	8.1	21.4
17	20.5	20.5	3.6	6.7	36.9
18	20.5	20.5	7	8.1	21.4
19	14.6	20.5	7	6.6	33.5
20	20.5	20.5	10.4	8.2	26.1

Table 5. The DOE simulation results for 3-layer 8/6 SRM with α=5°

Run order	Stator pole arc [deg.]	Rotor pole arc [deg.]	Turn on angle [deg.]	Average torque [N.m]	Torque ripple [%]
1	24	17	9	12.6	17.9
2	20.5	14.6	7	10.1	20.4
3	20.5	20.5	7	12.1	18.1
4	20.5	20.5	7	12.1	18.1
5	20.5	20.5	7	12.1	18.1
6	17	17	9	11.2	18.7
7	20.5	20.5	7	12.1	18.1
8	24	17	5	11.2	21.7
9	24	24	9	11.9	21.1
10	20.5	26.4	7	12.2	20
11	26.4	20.5	7	12.7	17.9
12	17	24	9	11.8	16.7
13	17	17	5	8.2	26.6
14	17	24	5	10.7	18.5
15	24	24	5	12.6	15.8
16	20.5	20.5	7	12.1	18.1
17	20.5	20.5	3.6	10	19.6
18	20.5	20.5	7	12.1	18.1
19	14.6	20.5	7	9.9	17.1
20	20.5	20.5	10.4	12.3	19.4

Table 6. The DOE simulation results for 4-layer 8/6 SRM with α=3.75°

Run order	Stator pole arc [deg.]	Rotor pole arc [deg.]	Turn on angle [deg.]	Average torque [N.m]	Torque ripple [%]
1	24	17	9	16.7	12.3
2	20.5	14.6	7	13.5	13.3
3	20.5	20.5	7	16.2	12.2
4	20.5	20.5	7	16.2	12.2
5	20.5	20.5	7	16.2	12.2
6	17	17	9	15	14.3
7	20.5	20.5	7	16.2	12.2
8	24	17	5	15	12
9	24	24	9	15.8	14.2
10	20.5	26.4	7	16.2	13.2
11	26.4	20.5	7	17	14.1
12	17	24	9	15.7	15.7
13	17	17	5	10.9	18
14	17	24	5	14.4	14.7
15	24	24	5	16.8	15.8
16	20.5	20.5	7	16.2	12.2
17	20.5	20.5	3.6	13.3	18.4
18	20.5	20.5	7	16.2	12.2
19	14.6	20.5	7	13.2	17.3
20	20.5	20.5	10.4	16.4	15.4

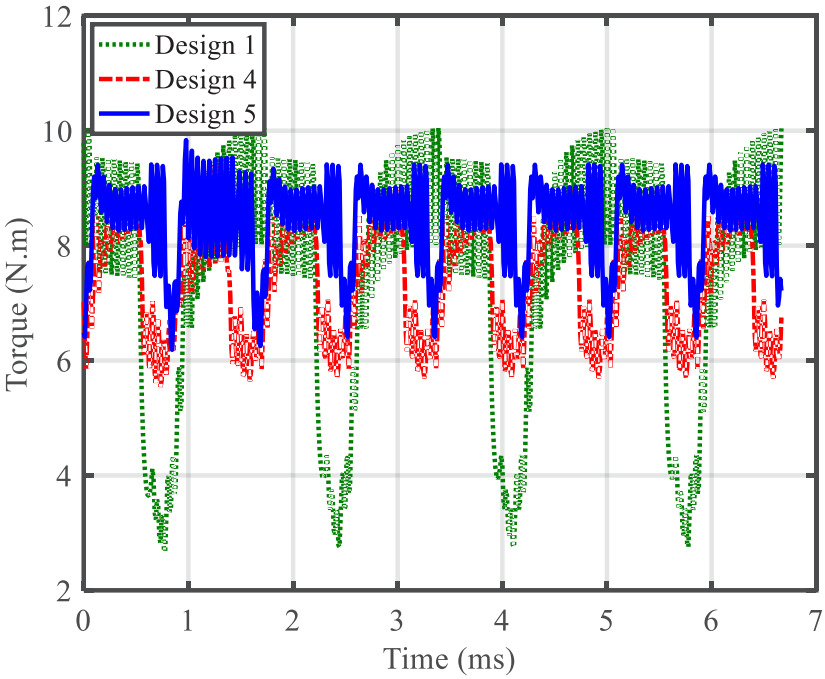

Fig. 9. Instantaneous torque of the 2-layer 8/6 SRM

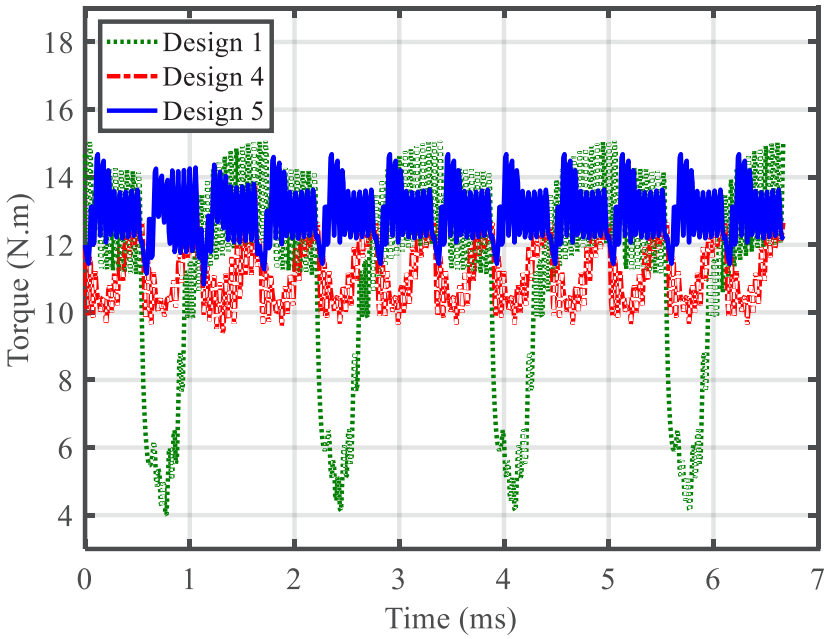

Fig. 10. Instantaneous torque of the 3-layer 8/6 SRM

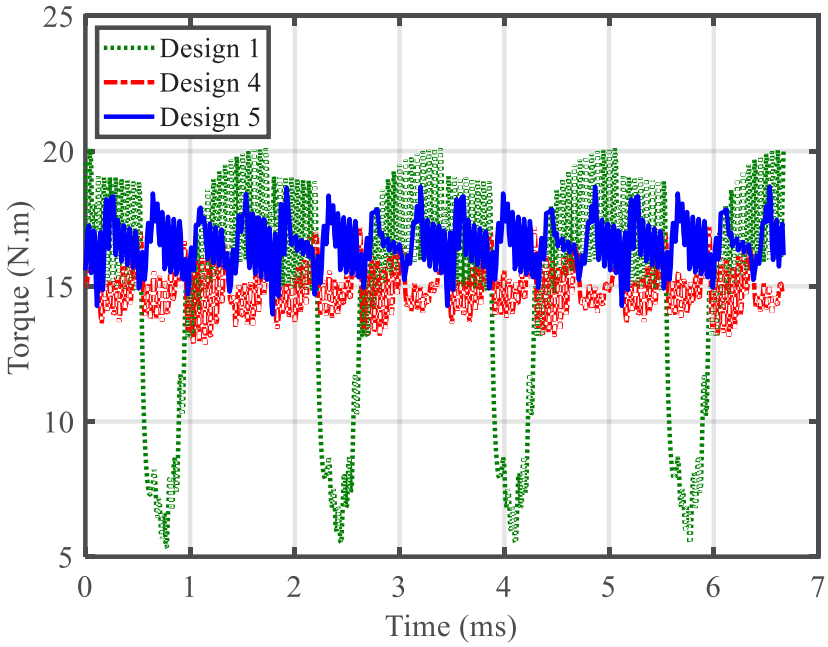

Fig. 11. Instantaneous torque of the 4-layer 8/6 SRM

Table 7. Simulation results for the second method

		Design 1	Design 4	Design 5
2-layer SRM	Average torque [N.m]	7.4	7.4	8.4
	Torque ripple [%]	49.7	26.5	21.7
3-layer SRM	Average torque [N.m]	11.1	11.1	12.9
	Torque ripple [%]	49.7	19.7	15
4-layer SRM	Average torque [N.m]	14.8	14.8	16.6
	Torque ripple [%]	49.7	14.6	14.2

Table 8. Simulation results when the first method is applied to the considered multi-layer 6/4 SRM

		Design 1	Design 2	Design 3
2-layer SRM	Average torque [N.m]	7.1	8.2	8.2
	Torque ripple [%]	76.1	30.6	19.4
3-layer SRM	Average torque [N.m]	10.6	12.3	12.3
	Torque ripple [%]	76.1	30.6	15.9
4-layer SRM	Average torque [N.m]	14.2	16.4	16.4
	Torque ripple [%]	76.1	30.6	14.5

4- Conclusion

By changing the geometric structure and determining the optimum values of some design/control parameters using the DOE algorithm, an effective design optimization method was introduced for the multi-layer SRM by which torque ripple is reduced significantly and average torque is also increased. Depending on the sequence of implementation of the two above-mentioned design optimization procedures, two different design optimization methods were introduced. Applying these two methods to a multi-layer 8/6 SRM with different numbers of layers, many simulation results based on the 2D finite element method using the ANSYS finite element package were presented. These simulation results showed a significant reduction of torque ripple while average torque was increased. One of the main drawbacks of the SRM is the high torque ripple. As a result, the proposed design optimization method can be considered as an effective design method for torque ripple reduction. Since average torque is also increased for the multi-layer SRM with a higher number of layers, this point can be utilized for the construction of a high-power SRM with minimum torque ripple.

References

[1] T. J. E. Miller, "Switched reluctance motor and their control," Oxford U. K. Clarendon, 1993.

[2] R. Krishnan, "Switched reluctance motor drives modeling, simulation, analysis, design and applications," CRC Press, FL, USA, 2001.

[3] Y. Hu and et al., "Winding-centre-tapped switched reluctance motor drive for multi-source charging in electric vehicle applications," IET Power Electron., vol. 8, no. 11, pp. 2067-75, 2015.

[4] X. D. Xue and et al., "Switched reluctance generators with hybrid magnetic paths for wind power generation," IEEE Trans. Magn., vol. 48, no. 11, pp. 3863-66, 2012.

[5] R. Todd and et al., "Behavioural modelling of a switched reluctance motor drive for aircraft power systems," IET Electr. Syst. Transp., vol. 4, no. 4, pp. 107-113, 2014.

[6] D. Choi, S. Byun and Y. Cho, "A study on the maximum power control method of switched reluctance generator for wind turbine," IEEE Trans. Magn., vol. 50, no. 1, pp. 1-4, 2014.

[7] J. P. Hong, K. H. Ha, and J. Lee, "Stator pole and yoke design for vibration reduction of switched reluctance motor," IEEE Trans. Magn., vol. 38, no. 2, pp. 929-932, 2002.

[8] J. Li, X. Song, and Y. Cho, "Comparison of 12/8 and 6/4 switched reluctance motor: noise and vibration aspects," IEEE Trans. Magn., vol. 44, no. 11, pp. 4131-34, 2008.

[9] J. O. Fiedler, K. Kasper, R. W. DeDoncker, "Calculation of the acoustic noise spectrum of SRM using modal superposition," IEEE Trans. Ind. Electron., vol. 57, no. 9, pp. 2939-2949, 2010.

[10] S. M. Castano, B. Bilgin, E. Fairall, and A. Emadi, "Acoustic noise analysis of a high-speed high-power switched reluctance machine: frame effects," IEEE Trans. Energy Convers., vol. 31, no. 1, pp. 69 –77, 2016.

[11] N. K. Sheth and K. R. Rajagopal, "Optimum pole arcs for a switched reluctance motor for higher torque with reduced ripple," IEEE Trans. Magn., vol. 39, no. 5, pp. 3214-16, 2003.

[12] B. Mirzaeian, M. Moallem, V. Tahani and C. Lucas, "Multiobjective optimization method based on a genetic algorithm for switched reluctance motor design," IEEE Trans. Magn., vol. 39, no. 5, pp. 3334-36, 2003.

[13] W. Wu, J. B. Dunlop, S. J. Collocott and B. A. Kalan, "Design optimization of a switched reluctance motor by electromagnetic and thermal finite-element analysis," IEEE Trans. Magn., vol. 39, no. 5, pp. 3334-36, 2003.

[14] A. M. Omekanda, Y. Kano, T. Kosaka and N. Matsui, "Robust torque and torque-per-inertia optimization of a switched reluctance motor using the Taguchi methods," IEEE Trans. Ind. Appl., vol. 42, no. 2, pp. 473-78, 2006.

[15] F. Daldaban and N. Ustkoyuncu, "Multi-layer switched reluctance motor to reduce torque ripple," Energ. Convers. Manage., vol. 49, pp. 974-79, 2008.

[16] Y. Kano, T. Kosaka and N. Matsui, "Optimum design approach for a two-phase switched reluctance compressor drive," IEEE Trans. Ind. Appl., vol. 46, no. 3, pp. 955-64, 2010.

[17] X. D. Xue, K. W. E. Cheng, T. W. Ng and N. C. Cheung, "Multi-objective optimization design of in-wheel switched reluctance motors in electric vehicles," IEEE Trans. Ind. Electron., vol. 57, no. 9, pp. 2980-87, 2010.

[18] D. H. Lee, T. H. Pham and J. W. Ahn, "Design and operation characteristics of four-two pole high-speed SRM for torque ripple reduction," IEEE Trans. Ind. Electron., vol. 60, no. 9, pp. 3637-43, 2013.

[19] T. Ishikawa, Y. Hashimoto and N. Kurita, "Optimum design of a switched reluctance motor fed by asymmetric bridge converter using experimental design method," IEEE Trans. Magn., vol. 50, no. 2, Article number: 7019304, 2014.

[20] C. Ma and L. Qu, "Multiobjective optimization of switched reluctance motors based on design of experiments and particle swarm optimization," IEEE Trans. Energy Convers., vol. 30, no. 3, pp. 1144-53, 2015.

[21] H. Cheng, H. Chen and Z. Yang, "Design indicators and structure optimisation of switched reluctance machine for electric vehicles," IET Electr. Power App., vol. 9, no. 4, pp. 319-31, 2015.

[22] B. Anvari, H. A. Toliyat and B. Fahimi, "Simultaneous optimization of geometry and firing angles for In-wheel switched reluctance motor drive," IEEE Trans. Transport. Electrific., vol. 4, no. 1, pp. 322-29, 2018.

[23] P. Vahedi, B. Ganji, and E. Afjei, "Multi-layer switched reluctance motors: performance prediction and torque ripple reduction," Int. Trans. Electr. Energ. Syst., vol. 30, no. 2, Article number: e12215, 2020.

[24] W.Y. Fowlkes and C.M. Creveling "Engineering methods for robust product design," Prentice Hall, 1995.

[25] J. Faiz, B. Ganji, C. E. Carstensen, and R. W. De Doncker, "Loss prediction in switched reluctance motors using finite element method," Int. Trans. Electr. Energ. Syst., vol. 19, pp. 731-48, 2009.

HOW TO CITE THIS ARTICLE

P. Vahedi, B. Ganji, E. Afjei, Design Optimization of the Multi-layer Switched Reluctance Motor to Minimize Torque Ripple and Maximize Average Torque, AUT J Electr Eng, 56(1) (Special Issue) (2024) 95-112.

DOI: 10.22060/eej.2023.22129.5518